Protein Science (1994), *3*:257-266. Cambridge University Press. Printed in the USA.

Real-time DNA binding measurements of the ETS1 recombinant oncoproteins reveal significant kinetic differences between the p42 and p51 isoforms

ROBERT J. FISHER,[1] MATTHEW FIVASH,[2] JOSE CASAS-FINET,[3] JOHN W. ERICKSON,[3] AKIKO KONDOH,[1] SHARON V. BLADEN,[1] CONSTANCE FISHER,[4] DENNIS K. WATSON,[4,5] AND TAKIS PAPAS[4,5]

[1] Laboratory of Cellular Biochemistry, PRI/DynCorp, National Cancer Institute-Frederick Cancer Research and Development Center, Frederick, Maryland 21702
[2] Data Management Services, Inc., National Cancer Institute-Frederick Cancer Research and Development Center, Frederick, Maryland 21702
[3] Frederick Biomedical Supercomputing Center, PRI/DynCorp, National Cancer Institute-Frederick Cancer Research and Development Center, Frederick, Maryland 21702
[4] Laboratory of Molecular Oncology, National Cancer Institute, Frederick, Maryland 21702

(RECEIVED August 3, 1993; ACCEPTED November 17, 1993)

Abstract

The sequence-specific DNA binding of recombinant p42 and p51 ETS1 oncoprotein was examined quantitatively to determine whether the loss of the Exon VII phosphorylation domain in p42 ETS1 or the phosphorylation of expressed Exon VII in p51 ETS1 had an effect on DNA binding activity. The kinetics of sequence-specific DNA binding was measured using real-time changes in surface plasmon resonance with BIAcore (registered trademark, Pharmacia Biosensor) technology. The real-time binding of p42 and p51 ETS1 displayed significant differences in kinetic behavior. p51 ETS1 is characterized by a fast initial binding and conversion to a stable complex, whereas p42 ETS1 exhibits a slow initial binding and conversion to a stable complex. All of the p51 ETS1 DNA binding states are characterized by rapid turnover, whereas the p42 ETS1 DNA binding states are 4-20 times more stable. A model describing these kinetic steps is presented. Stoichiometric titrations of either p42 or p51 ETS1 with specific oligonucleotides show 1:1 complex formation. The DNA sequence specificity of the p42 and p51 ETS1 as determined by mutational analysis was similar. The in vitro phosphorylation of p51 ETS1 by CAM kinase II obliterates its binding to specific DNA, suggesting that the regulation of p51 ETS1 sequence-specific DNA binding occurs through phosphorylation by a calcium-dependent second messenger. The p42 ETS1 lacks this regulatory domain (Exon VII), and binding to its specific DNA sequence is not sensitive to calcium signaling.

Keywords: BIAcore; CAM kinase II; DNA binding; p42 ETS1; p51 ETS1; sequence-specific binding; surface plasmon resonance

The *ets* oncogene of the E26 retrovirus defines a family of conserved cellular genes whose gene products are capable of binding to a purine-rich DNA sequence (Gegonne et al., 1992; Seth et al., 1992) and transactivation of heterologous promoters (Ho et al., 1990). The regulation of the ETS DNA binding activity has been a subject of considerable interest for several reasons. At the structural level, it is evident that the 85-amino acid ETS DNA binding domain does not have homology to known DNA binding motifs and could represent a new DNA binding fold (Mavrothalassitis et al., 1994). From the biological perspective, the ETS binding domain defines a large family of related proteins that are recruited to a specific promoter by a mechanism(s) still unknown. All of the ETS family factors recognize a similar GGA core DNA sequence (Fisher et al., 1991; Nye et al., 1992), but must find specificity in the flanking DNA sequences to the GGA core or must interact with other proteins to obtain specificity for a particular member of the ETS family. Several different modes of interaction with DNA have been described

Reprint requests to: Robert Fisher, Bldg. 469, Rm. 230, NCI-Frederick Cancer Research and Development Center, P.O. Box B, Frederick, Maryland 21702-1201; e-mail: fisher@fcrfv1.ncifcrf.gov.

[5] Present address: Center for Molecular and Structural Biology, Hollings Oncology Center, Medical University of South Carolina, 171 Ashley Avenue, Charleston, South Carolina 29425.

Abbreviations: CAM, calmodulin-dependent protein; EMSA, electrophoretic mobility shift assay; ITPG, isopropylthio-β-galactoside; OPC, oligonucleotide purification column; SPR, surface plasmon resonance; RU, resonance unit; BIAcore, registered trademark, Pharmacia Biosensor; NHS, *N*-hydroxysuccinimide; TFA, trifluoroacetic acid.

for ETS family members, so it is not yet possible to generalize a mechanism that would be characteristic for ETS-related proteins. Thus, there are at least 8 distinct mechanisms described: (1) formation of a noncovalent ternary complex (Wasylyk et al., 1990); (2) phosphorylation-dependent formation of a transcriptionally active ternary complex (Hill et al., 1993); (3) phosphorylation-dependent formation of a ternary complex (Pongubala et al., 1993); (4) formation of a heterodimer–DNA complex (Thompson et al., 1991); (5) change in the primary structure of an ETS protein by use of alternatively spliced mRNA (Fisher et al., 1992); (6) DNA binding regulated by the phosphorylation state of the ETS1 protein (Pognonec et al., 1990); (7) intramolecular regulation of DNA binding (Hagman & Grosschedl, 1992; Lim et al., 1992; Wasylyk et al., 1992); and (8) formation of a noncovalent ternary complex of 2 ETS-related proteins (Nelson et al., 1993).

We have shown that the human ETS1 oncoprotein found in T-cell leukemia cell lines (CEM and Jurkat) exists in 2 forms as a result of alternate splicing of the mRNA (Koizumi et al., 1990; Jorcyk et al., 1991; Fisher et al., 1992). The p51 isoform is the full-length ETS1, as determined by N-terminal amino acid sequencing, amino acid analysis, and anti-peptide antibodies (Fisher et al., 1992), whereas the p42 isoform is lacking the amino acids corresponding to Exon VII (Jorcyk et al., 1991). Exon VII is a regulatory domain of the ETS1 protein because it is the site of phosphorylation by a calcium-dependent protein kinase (Koizumi et al., 1990; Fleischman et al., 1993). The p51 ETS1 is phosphorylated in response to external stimuli, whereas the p42 ETS1 is not. Thus far, the significance of this phosphorylation has been explored only in cycling cells, where hyperphosphorylation is found during mitosis (Fleischman et al., 1993).

Studies of sequence-specific DNA binding have used the sensitive but cumbersome technique of the electrophoretic mobility shift assay, which is very good for identification of DNA–protein complexes but can only provide limited kinetic data. Quantitative EMSA analysis of renatured ETS1 from CEM cells showed little difference in their K_a values between the optimal DNA binding sequence and mutant 3, but did show a difference in stability of the DNA–protein complexes. The optimal DNA binding sequence gave a $t_{1/2}$ of 13.4 min and with the mutant 3 DNA gave a $t_{1/2}$ of 5.1 min (Fisher et al., 1991). We therefore chose direct, real-time measurements of protein–DNA complex formation employing surface plasmon resonance and BIAcore technology so that we could define the kinetic pathway for the DNA sequence-specific binding of p42 and p51 ETS1 to short oligonucleotides. These data were fit to a kinetic model that helps to elucidate differences in the kinetic pathway that the p42 and p51 use to achieve their binding. We then used this technique to scan DNA point mutations through the 9-bp recognition site. For the purpose of comparison, we also measured the stoichiometric binding of ETS1 to specific oligonucleotides using changes in tryptophan fluorescence. In this publication, we show that both p51 and p42 ETS1 bind to DNA with high affinity and form a 1:1 stoichiometric complex with their specific DNAs, that kinetic measurements show dramatic differences in the kinetic pathway used to obtain stable binding, and that phosphorylation of the p51 ETS1 causes loss of DNA sequence-specific binding. We introduce the use of the BIAcore methodology for the kinetic measurement of protein binding to DNA, and show that this instrumentation allows discovery of detail in the binding process that would be elusive by any other method.

Results

EMSA of renatured p42 and p51 ETS1

The data in Figure 1A show that both the p42 (lanes 1–6) and the p51 (lanes 7–12) ETS1 are capable of retarding all of the added specific oligonucleotide, providing that enough protein is added. The size of the p42–DNA complex is slightly smaller than the size of the p51–DNA complex. As shown in Figure 1B (lanes 4–6), both the p42 and the p51 isoforms have the same DNA specificity, not binding at all to mutations in the GGA core. This shows that both the p42 and p51 ETS1 proteins form discrete stable complexes with their specific DNA and display a similar pattern of specificity with point-mutated oligonucleotides. To probe the kinetic pathway of protein–DNA complex formation, we used real-time measurement of complex formation.

BIAcore measurement of DNA–protein interaction

The BIAcore is a biosensor-based device that measures SPR, which detects changes in properties at the surface of a thin gold film on a glass support (Lofas & Johnsson, 1990). The sensor surface is a removable chip modified with carboxymethylated dextran to which streptavidin is covalently attached. This surface can then capture biotinylated canonical or mutant oligonucleotides. The surface is particularly well suited to study DNA because once attached by the biotin–streptavidin, the DNA backbone is repelled from the carboxymethylated surface, allowing space for the interacting protein. The chip is mounted in a flow cell, and a solution bearing the protein is passed over the chip at a defined flow rate; binding causes a change in SPR that is detected optically and is measured in arbitrary units, resonance units. An example of the sequence-specific DNA binding of p42 and p51 ETS1 measured by BIAcore technology is shown in Figure 2. It is evident from inspection of the 2 curves that there is a significant difference in the shape and, therefore, the kinetics of DNA binding as measured in the BIAcore instrument for these 2 similar proteins. These shape differences are primarily determined by the protein–DNA reaction pathway rather than differing machine response, because the introduction of a single point mutation in position 4, a G to A change (GCCGGAAGT to GCCG**A**AAGT), essentially eliminates the binding of both p42 and p51 ETS1. The small deflection when the protein is passed across the mutant surface is due to slight differences in buffer composition and pressure changes during the injection from the sample loop. The results shown in Figure 1A demonstrate that the steady-state level of sequence-specific binding is very similar and that the sequence specificity of p42 and p51 is similar (Fig. 1B). BIAcore analysis of real-time binding shows a difference in the kinetic pathway to achieve steady-state binding. The low noise and high sensitivity of this measurement method provide additional details about possible contact residues in the flanking bases surrounding the canonical GGA core. The data in Figure 3 summarize the relative binding of p42 and p51 ETS1 to oligonucleotides mutated in each position of the specific site (the same oligonucleotides as shown in Fig. 1B). The EMSA results indicating that mutations at positions 4, 5, and 6 (the GGA core) abolish binding are confirmed by the BIAcore experiments (Fig. 3). It is possible that these bases are in direct contact with the most conserved amino acids

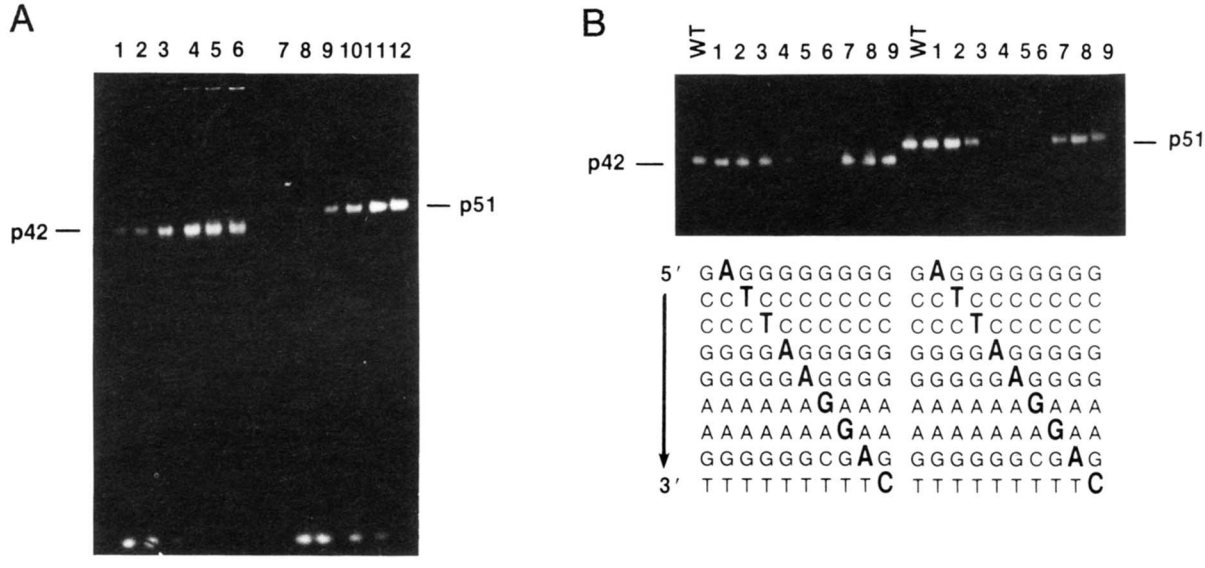

Fig. 1. A: Constant amount of wild-type probe, 1.0 μM (250 ng/20μL), titrated with increasing amounts of p42 ETS1 (lanes 1–6) or p51 ETS1 (lanes 7–12). The amounts of p42 used were 1.0 μM (855 ng/20 μL), 2.0 μM (1,710 ng/20 μL), 3.9 μM (3,420 ng/20 μL), 7.9 μM (6,840 ng/20 μL), 9.8 μM (8,550 ng/20 μL), and 15.8 μM (13,680 ng/20 μL) in lanes 1–6, respectively, and the amounts of p51 were 0.3 μM (324 ng/20 μL), 0.6 μM (648 ng/20 μL), 1.2 μM (1,296 ng/20 μL), 2.4 μM (2,592 ng/20 μL), 3.0 μM (3,240 ng/20 μL), and 4.9 μM (5,184 ng/20 μL) in lanes 7–12, respectively. **B:** Binding of 3.9 μM p42 ETS1 (3,420 ng/20 μL, left-hand side) or 3.0 μM p51 ETS1 (3,240 ng/20 μL, right-hand side) with 1.0 μM (250 ng/20 μL) of wild-type (WT) DNA or with 1.0 μM (250 ng/20 μL) of point-mutated DNA (1–9). The core DNA sequence is shown below each lane, and the mutated base is shown in bold.

of the ETS1 DNA binding domain (Mavrothalassitis et al., 1994). The BIAcore method reveals additional evidence that bases at positions 1, 7, and 9 may also be contact residues. The data in Table 1 show the apparent association constants for each mutation along with the half-lives of the mutant DNA–ETS1 complexes. The p42 ETS1 has a reduced half-life or does not bind to all of the mutants except for mutant 8, which makes a more stable complex. The $K_{a(app)}$ for all of these complexes are at least 10-fold lower than with the p42 complex with the wild-type DNA. By contrast, several of the mutant DNAs (mutants

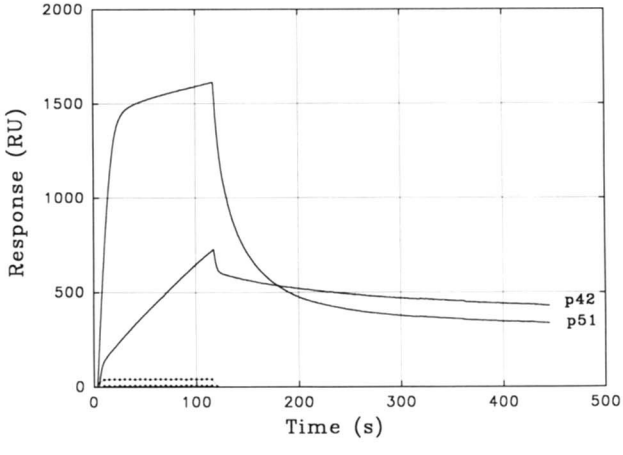

Fig. 2. Binding response of p51 and p42 protein on wild-type (GCCGGAAGTG) and mutant 4 (GCCAGAAGT) DNA. There were 687 RUs of wild-type DNA and 470 RUs of mutant 4 DNA attached to the sensor surface. The solid lines represent the RU response to the wild-type DNA, and the dotted lines represent the RU response to mutant 4 DNA. The small response to mutant 4 DNA is due to pressure changes in the flow cell at protein injection. The flow concentration is 0.0057 g/L (110 nM) for p51 and 0.00378 g/L (90 nM) for p42.

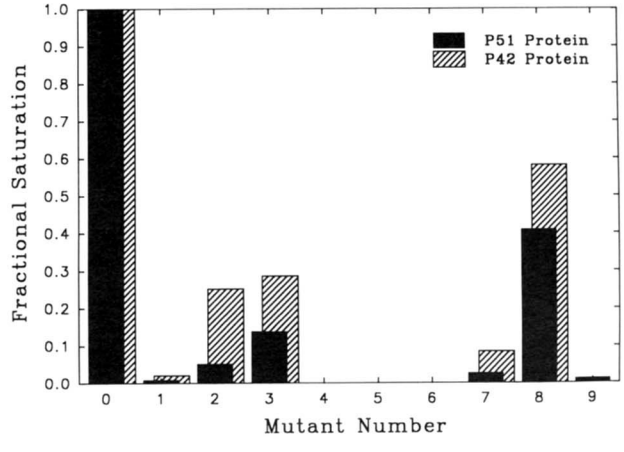

Fig. 3. Apparent binding capacity for the set of single-base DNA mutations in the binding domain as a percentage of the actual binding capacity (fractional saturation). $R_{max(app)}$ is determined through the experimental Langmuir equivalence defined in the text. There were 813 RUs of mutant 1, 427 RUs of mutant 2, 738 RUs of mutant 3, 470 RUs of mutant 4, 621 RUs of mutant 5, 870 RUs of mutant 6, 605 RUs of mutant 7, 602 RUs of mutant 8, 429 RUs of mutant 9, and 746 RUs of wild-type DNA (mutant 0) attached to the sensor surface. The stock solutions of p51 and p42 were 1.1 and 9 μM, respectively, and a 20-μL injection (8 μL/min) of 1:10, 1:25, 1:50, 1:100, 1:250, and 1:500 passed through the flow cell.

Table 1. *Binding of p51 and p42 to wild-type and mutant DNA*

DNA	p51		p42	
	K_{equ} (M^{-1})	$t_{1/2}$ (s)	K_{equ} (M^{-1})	$t_{1/2}$ (s)
Wild type	$1.41 \cdot 10^8 \pm 4.3 \cdot 10^6$[a]	277	$2.80 \cdot 10^8 \pm 4.4 \cdot 10^6$	1,155
Mutant 1	$1.30 \cdot 10^8 \pm 3.5 \cdot 10^6$	266	$2.71 \cdot 10^8 \pm 3.8 \cdot 10^6$	500
Mutant 2	$6.63 \cdot 10^7 \pm 1.4 \cdot 10^6$	469	$3.12 \cdot 10^7 \pm 1.8 \cdot 10^5$	878
Mutant 3	$9.96 \cdot 10^6 \pm 1.2 \cdot 10^5$	496	$1.85 \cdot 10^7 \pm 2.2 \cdot 10^5$	965
Mutant 4	$<1 \cdot 10^5$ –	–	$<1 \cdot 10^5$ –	–
Mutant 5	$<1 \cdot 10^5$ –	–	$<1 \cdot 10^5$ –	–
Mutant 6	$<1 \cdot 10^5$ –	–	$<1 \cdot 10^5$ –	–
Mutant 7	$1.36 \cdot 10^7 \pm 2.1 \cdot 10^5$	198	$1.79 \cdot 10^7 \pm 2.4 \cdot 10^5$	565
Mutant 8	$5.43 \cdot 10^8 \pm 2.2 \cdot 10^6$	1,579	$5.63 \cdot 10^7 \pm 5.4 \cdot 10^5$	1,216
Mutant 9	$6.71 \cdot 10^8 \pm 1.65 \cdot 10^7$	165	$<1 \cdot 10^5$ –	–

[a] Absolute value = standard error.

2, 3, and especially 8) form a more stable complex with p51 ETS1.

In vitro phosphorylation of p51 ETS1 and specific interaction with DNA

We tested whether phosphorylation could alter the specific interaction of p51 with DNA. We have shown that Exon VII encodes for a site that is phosphorylated by a calcium-dependent protein kinase; the site and Exon VII are missing in p42 and it does not become phosphorylated (Koizumi et al., 1990). As is shown in Figure 4, the phosphorylation of p51 by CAM kinase II inhibits sequence-specific DNA binding, whereas no effect of CAM kinase II is observed on the DNA sequence-specific binding of p42. The phosphorylation of p51 ETS1 reduces the $K_{a(app)}$ by 14-fold, which is sufficient to dramatically reduce binding to the optimized ETS1 site. These data strongly suggest that the DNA sequence-specific binding of p51 ETS1 is regulated by calcium-dependent phosphorylation and that the p42 sequence-specific DNA binding is independent of calcium signaling. The details of the identification of the location of the serine residue in Exon VII that becomes phosphorylated will appear elsewhere (Fisher, in prep.).

Kinetic model of the specific interaction of ETS1 with DNA

Examination of the real-time binding curves for the specific interaction of p42 and p51 ETS1 shows that the binding curves are different. To understand and elaborate these differences, we have proposed the kinetic model shown in Figure 5. The model shows diffusion-limited movement of the protein from the flow into a free (unbound) compartment within the dextran surface; here there is a rapid sequence-specific DNA binding (B_1) followed by conversion through (B_2) into the stably bound species (B_3). A graphical examination of the measurements shows how

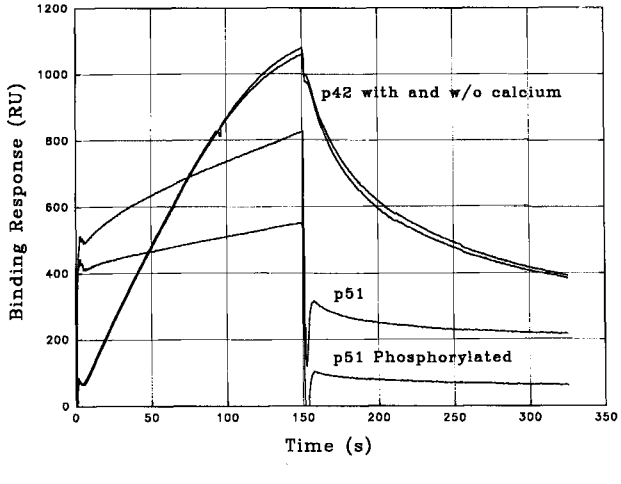

Fig. 4. All of the components necessary for the CAM kinase II phosphorylation were present, and the phosphorylation was initiated by addition of calcium. The controls used calcium plus EGTA as described in Materials and methods. The sensor surface had 745 RUs of DNA attached. The flow concentration was 0.0057 g/L for p51 (110 nM) and 0.00378 g/L (90 nM) for p42.

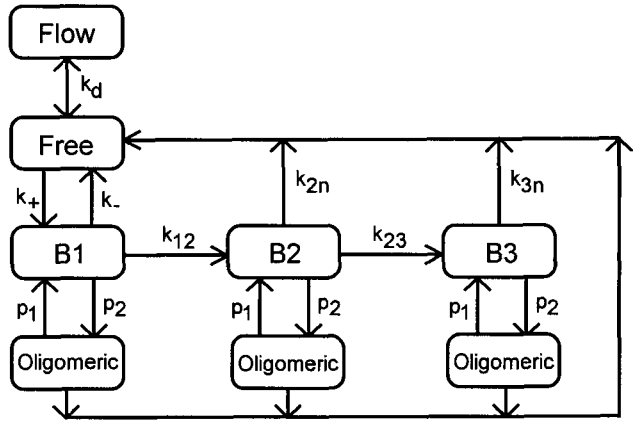

Fig. 5. Compartmental diagram of the model used to analyze the binding of p51 and p42 to wild-type DNA. The equation describing this model (Equation 1) is shown in the text. This model is not strictly a "compartmental" model; however, the diagram shows the way our model accounts for the various complex types in the binding reaction.

our model relates to the binding reaction. The data in Figure 2 show the binding of p51 protein to wild-type DNA and the response of p51 to mutant DNA. Note that there is very little RU response to the mutant DNA, showing that the large, fast rise in the RU signal on the wild-type surface is due to site-specific protein–DNA interaction. The rapid rise in the RU signal is rate-limited by diffusion. The following slow increase in the RU signal is due primarily to conversion of the B_1 complex to the B_3 complex. Examination of the washout phase shows 3 distinct exponential decays: a rapid decay of the quickly changing B_1 complex followed by a rounding due to the slower moving B_2 complex and finally the very slow decay of the B_3 complex. These 3 significant states in the binding reaction form the basis of our proposed model. This model is the simplest description that is consistent with the physical assumptions of a stochastic stationary state (equilibria) of the binding reaction and operation of the instrument (machine effects) that will describe our measurements over the complete time course and concentration series of a binding experiment. The model (Fig. 5) accounts for the overall time course, both for protein flow and washout, of the observed binding of both the p42 and p51 ETS1 proteins to the specific DNA site as the protein concentration is varied. The kinetic parameters in Table 2 for p51 (Kinemage 1) and p42 (Kinemage 2) isoforms show how the very different time progressions of binding for these 2 proteins are related. Our model predicts that, at equilibrium, both p42 and p51 will bind a significant portion of the available sites, a prediction verified by classical EMSA experiments (Fig. 1A) and stoichiometric titrations. The movement of p51 ETS1 through these binding states is shown in Figure 6A and B. The B_1 binding phase for p51 is rapid, and within a second or two is already moving into the B_2 state and begins converting into the B_3 state. After 16 min, p51 ETS1 is distributed equally among all 3 binding states. The fast turnover of the p51 ETS1 B_3 (4.6 min) limits the buildup of p51 ETS1 in B_3. In contrast, the p42 binding in Figure 2 shows a limited B_1 response followed by a steady increase in the RU signal that is primarily due to conversion of the B_1 complex to the B_3 complex. The movement of p42 ETS1 through these binding states is shown in Figure 6C and D, where the B_1 and B_2 response is weak because of the slow turnover of B_3 (19.3 min). That is, the loss of Exon VII overcomes the kinetic instability of the p51 ETS1–DNA complex.

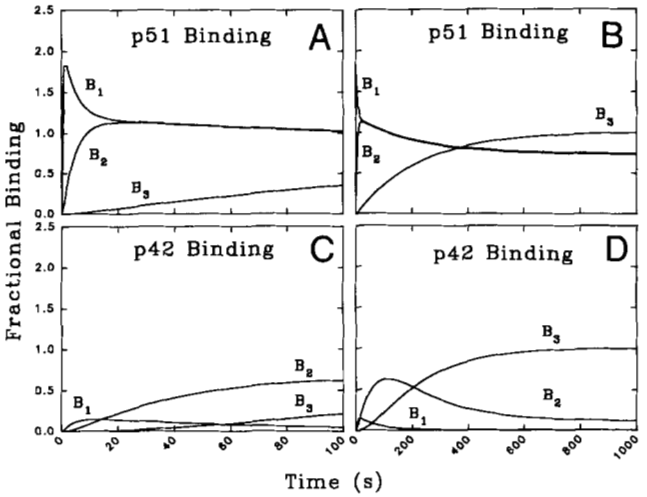

Fig. 6. Differences in DNA binding of p42 and p51 protein shown as fractional binding of their respective B_3 states. **A:** First 100 s of p51 binding. **B:** p51 binding out to 1,000 s. **C:** First 100 s of p42 binding. **D:** p42 binding out to 1,000 s. The sensor surface has 39 RUs of wild-type DNA attached. Stock solutions of p51 and p42 were 1.1 and 9 μM, respectively, and a 20-μL injection (8 μL/min) of 1:10, 1:25, 1:50, 1:100, 1:250, and 1:500 passed through the flow cell.

Fluorimetric titrations

To provide evidence for the stoichiometry of the p42 and p51 ETS1 interaction with specific oligonucleotides and to have an estimation of the apparent association constant by an independent method, fluorimetric studies were undertaken. The ETS1 tryptophan fluorescence emission was quenched monotonically with increasing amounts of oligonucleotide until a level was reached after which no further quenching was observed (not shown). This behavior is characteristic of tight (stoichiometric) ligand binding; it allowed the calculation of the limiting quenching ($Q_{max} = 0.365$) from the plateau level and of the binding stoichiometry (1.1 ± 0.1 oligonucleotide molecules/p51 monomer) from the intersection with the plateau of the initial slope. Binding affinities could not be calculated, however, as practically no free ligand was present at equilibrium at the stoichio-

Table 2. *Parameters for p51 and p42 binding to wild-type (WT) DNA*

Parameter	WT DNA-p51 binding	WT DNA-p42 binding
Diffusion	1.9 L s^{-1} mm^{-2} ± 0.30[a]	1.6 L s^{-1} mm^{-2} ± 0.03
B_1 association	949 mm^2 g^{-1} s^{-1} ± 207	10.8 mm^2 g^{-1} s^{-1} ± 0.45
B_1 disassociation	1.30 s^{-1} ± 0.33	0.15 s^{-1} ± 0.02
B_1 to B_2 conversion	0.13 s^{-1} ± 0.03	0.10 s^{-1} ± 0.007
B_2 disassociation	0.13 s^{-1} ± 0.010	0.001 s^{-1} ± 0.00001
B_2 to B_3 conversion	0.004 s^{-1} ± 0.0003	0.0054 s^{-1} ± 0.0005
B_3 disassociation	0.003 s^{-1} ± 0.0002	0.0006 s^{-1} ± $8.3 \cdot 10^{-6}$
B_1 half-life	0.5 s	2.7 s
B_2 half-life	5.2 s	108 s
B_3 half-life	277 s	1,155 s
Flow concentration (undiluted)	$1.04 \cdot 10^{-6}$ M	$9.00 \cdot 10^{-6}$ M

[a] Absolute value = standard error.

metric point. Similar titrations were carried out at lower initial p51 concentrations to displace the equilibrium toward free ligand, according to the law of mass action. A double-reciprocal plot of a titration carried out at the lowest p51 concentration assayed (24 nM) yielded a Q_{max} of 0.375, in good agreement with that obtained from p51 titrations at micromolar concentrations, and a binding affinity of 2.9×10^8 M^{-1} in 10 mM Tris buffer containing 33 mM NaCl. Attempts to perform salt-back titrations on preformed ETS1-oligonucleotide complexes were unsuccessful in that no significant change of the complex fluorescence emission intensity was observed. This could be due to a kinetic block to complex dissociation or a nearly null dependence of K_{app} on salt concentration, among other causes. To circumvent this problem, we carried out titrations of p51 ETS1 protein with oligonucleotides at various (constant) NaCl concentrations. A double-logarithmic plot of $d(\log K)$ vs. $d(\log [Na^+])$ showed that, indeed, the salt dependence of the binding was very small, albeit measurable. It was found, however, that Q_{max} varied with salt concentration, attaining 0.636 for the highest [NaCl] assayed (4 M); this precluded the use of salt-back titrations with this system.

For the interaction of the p51 isoform of ETS1 with the annealed oligonucleotide containing its specific DNA sequence, we measured a $d(\log K)/d(\log [Na^+])$ of -0.43. In the absence of anion binding, p51 would displace less than 1 monovalent cation upon oligonucleotide binding. Such a low value suggests that anion uptake by p51 does occur upon oligonucleotide binding and that it nearly compensates for the cation release from the oligonucleotide lattice. This accounts for the very low salt dependence of binding affinity observed for p51, as the magnitude of the net ion uptake is almost null. Although a deconvolution of the relative contribution of the anion and cation binding could be obtained by investigating the dependence of the K_{app} with different salts, it lies outside the scope of this paper. Note, however, that p51 anion uptake of glutamate (the dominant anion in the intracellular environment) could be significantly different from that observed for chloride; macromolecular crowding and exclusion effects (affecting water activity coefficient) also should be considered before extrapolating to conditions in vivo.

We measured a nonelectrostatic contribution to the free energy of binding of -43 kJ mol^{-1} (10.2 kcal mol^{-1}) for the interaction of the p51 isoform of ETS1 with the specific oligonucleotide. Our results indicate that, at 0.1 M NaCl, ca. 95% of the oligonucleotide binding free energy originated from nonelectrostatic interactions.

For the p42 isoform of ETS1, binding to the specific oligonucleotide was also observed with a 1:1 stoichiometry. Interestingly, it resulted in an enhancement of the Trp fluorescence emission intensity, reaching a limiting value of 31% at saturation ($E_{max} = 1.31$). The K_{app} for the oligonucleotide was higher than that of the p51 isoform, as stoichiometric or near-stoichiometric binding was observed at all p42 concentrations except in the low nanomolar range. A lower limit for the affinity of p42 for the specific oligonucleotide was estimated at 1×10^9 M^{-1}. This represents an affinity roughly an order of magnitude higher than that of the p51 isoform. An accurate value would require extrinsic labeling of p42 with an appropriate fluorophore (e.g., fluorescein, rhodamine). As observed with p51, salt-back titrations did not affect the fluorescence emission intensity.

Discussion

We have used BIAcore technology to gain insight into the kinetic pathway of sequence-specific DNA binding for p42 and p51 ETS1. Aside from the ability of the BIAcore to make real-time binding measurements, the DNA surfaces on the sensor chip may be used throughout a particular experiment, allowing the direct comparison of p42 and p51 ETS1 binding to exactly the same DNA. To extract as much information as possible from the binding reactions, we have developed a minimal kinetic model that describes the data from a concentration series of p42 and p51 ETS1 covering 2 orders of magnitude.

Analysis, in terms of a model, is a useful method for understanding the measurements recorded by the BIAcore instrument. We begin by assuming that the binding system is characterized by a macroscopic equilibrium, that is, there is an equilibrium state in which the amount of new complex formed equals the amount of complex disassociating in each unit of time (Lohman & Bujalowski, 1991; Record et al., 1991). This assumption, that the stochastic process of complex formation reaches a stationary state, leads to a family of systems of differential equations, the simplest of which is the well-known Langmuir rate equation on which the standard BIAcore analysis package is based.

Data recorded by the BIAcore instrument contain very little noise, permitting various mathematical models to be examined in detail for agreement with the measurements. A model that provides reasonable insight into the nature of a binding reaction must describe the entire time progression of the binding reaction (both injection and washout phases) as experimental parameters are varied. The effects of the measurement device need to be accounted for by the model so that a clear picture of the reaction itself can be obtained. The Langmuir model fails these requirements completely for our binding reaction. We recognize that the numerical difficulties of estimating parameters in systems of differential equations have led to suggestions for obtaining suboptimal parameter estimates, often based on the assumption of Langmuir kinetics. This requires selection of a subset of data that appears to follow Langmuir kinetics (e.g., BIAcore application notes). Any attempt to force fit the Langmuir model to such data obfuscates the nature of the kinetics and produces parameter estimates of questionable utility. When the binding kinetics does not follow the Langmuir model, fitting this model to a selected subset of data produces parameter estimates that cannot be expected, in general, to provide useful comparisons between different binding systems.

In addition to the assumption of a stochastic stationary state (equilibria), we assume that the model must be the same, possibly with different parameter values, for both p51 and p42 binding. This assumption is based on the observation that p42 is a shortened version of p51, and both proteins show similar sequence specificity, binding to the same 9-bp DNA sequence. We have found that the general time course of these binding reactions may be described by assuming that the bound complex exists in 1 of 3 states, which may be labeled B_1, B_2, and B_3. Several similar models have been suggested for binding reactions observed in other experimental settings (Andrade & Hlady, 1986). Less complex models, which may describe the time course of these experiments at 1 protein concentration, or a portion of the time course at several protein concentrations, lack the generality to describe a complete set of time progressions at several protein concentrations. The B_1 complex is modeled as exhibit-

ing directly reversible binding, whereas the B_2 and B_3 complexes are modeled as showing indirectly reversible binding. A compartmental drawing of the model is shown in Figure 5. The model describes the protein-protein interaction inferred from consideration of the maximum number of RUs of protein that could bind to the DNA if every site formed a complex. We show, in the kinemage file, data from a surface with only 39 RUs of DNA in the dextran matrix. At this low concentration of DNA, the individual DNA helices are widely separated so that interactions between neighboring receptor sites are unlikely. Sensor chip surfaces with concentrations of DNA greater than 150 RUs show increasingly significant steric hindrance effects. For the 39-RU surface, we find that more protein comes out of solution and attaches to the DNA on the surface than a 1:1 stoichiometry will allow. Examination of the RU response to dextran alone, and to dextran with streptavidin, shows that the protein does not bind to these surfaces. As the protein tends to form aggregates at high protein concentration (see Fig. 1A, lanes 4–6, where large aggregates are found on top of the gel), we include terms that allow for protein–protein interactions on the surface in our model. The fluorimetric titrations confirm earlier results indicating that ETS1 forms 1:1 complexes with the specific oligonucleotides (Fisher et al., 1992; Hagman & Grosschedl, 1992; Lim et al., 1992; Nye et al., 1992), thus the protein–protein interaction that we observe is due to piggyback aggregations or polymerization of protein that is already DNA bound. This interaction is weak and washes out when the ETS1-bearing solutions are changed to just buffer-containing solutions.

The model shown in Equations 1 and 2 might be compared with the Langmuir model by using an "experimental equivalence." In a classic equilibrium binding experiment, the B_3 complex would be predominantly observed after the separation step, as this complex degrades slowly. Taking the free ligand to be the flow concentration, a dilution series may be fit with the Langmuir rate equation using the measurements at the end of the washout phase of an experimental run. When the B_3 complex has a much slower off-rate than the other 2 complexes, and the washout phase is sufficiently long, the measurements during the last several seconds are predominantly determined by the B_3 complex. This approach, however, ignores any differences between the surface chemistry monitored by the BIAcore instrument and the volume chemistry generally associated with the application of Langmuir's equation to macromolecule binding phenomena. Further, our model does not reduce to the Langmuir rate equation in the case of the B_3 complex (or any of the other complexes), and thus a direct comparison of the rate constants is of uncertain value. While acknowledging these objections in comparing the Langmuir model with the one used here, "Langmuir equivalent" $K_{a(\text{app})}$ and $R_{\max(\text{app})}$ are calculated by this method. These values should be interpreted with care, especially when comparing values from reaction systems to which the Langmuir model applies. With the knowledge of these limitations, we have used this approach to compare the relative binding of p42 and p51 ETS1 to the mutant DNA surfaces shown in Figure 3 and Table 1 and to compare the relative binding of p51 and phosphorylated p51 to the specific ETS DNA binding site.

Free protein movement into the dextran matrix is modeled by Fick's diffusion law. Consideration of the flow cell shows that the assumptions of zero temperature gradient and laminar flow are reasonable. In this case, diffusion is primarily responsible for delivery of protein across the boundary layer to the surface. When there is no DNA in the dextran matrix, the time to equilibrium under diffusion is approximately 1.3 s for a flow of 8 μL min^{-1} (Lok et al., 1983). There is a large standard error in the B_1 association and B_1 dissociation (Table 2) because the model of diffusion is not complete, and this causes uncertainty in the B_1 estimations. However, some detailed structure in the measurements (i.e., "the pressure jump") is not described (see Kinemage 1, View 2), suggesting that there is further information to be recovered. When the amount of DNA in the dextran matrix is very low, it becomes less likely for the binding reaction to significantly influence the diffusion time, and the simplified model shown in Equation 1 provides a good description of the reaction system.

The regulation of sequence-specific DNA binding by p42 and p51 ETS1 is found to be multifaceted. Endpoint EMSAs demonstrate that the p42 and p51 ETS1 bind and form stable complexes with the optimal ETS binding site. The specificity of the DNA binding has not changed, because the p42 and p51 ETS1 have exactly the same pattern of binding on a series of DNA point mutations throughout the 9-bp binding site. The p42 and p51 ETS1 isoforms that are the products of alternatively spliced cDNAs qualitatively bind similarly to DNA. Using the BIAcore to access the kinetic pathway of DNA binding revealed interesting differences in how these 2 ETS isoforms bind to DNA. The p51 ETS1 was able to recognize and bind the specific DNA very rapidly, indicating the ability of this ETS1 form to efficiently find its specific binding site. In the absence of any other proteins or factors, the p51 ETS1 rapidly comes out of the B_1 state and is converted into B_2 and B_3 binding. The turnover of the p51 ETS1–DNA complexes is 4–20 times faster than the comparable p42 ETS1 DNA states. We propose that the p51 ETS1 forms less stable DNA complexes than does the p42 ETS1; interaction of the p51 ETS1 with other components of the transcriptional machinery (i.e., co-activators) (Liu et al., 1993), transcriptional associated factors (TAFS) (Pugh & Tjian, 1992), or even the TATA binding protein (TBP) (Nikolov et al., 1992; Zawel & Reinberg, 1993) itself may overcome this kinetic instability, allowing the p51 ETS1 to move rapidly into the B_3 stable binding. The sequence-specific DNA binding p51 ETS1 is also subject to additional regulation by calcium-dependent phosphorylation. The in vitro phosphorylation of p51 ETS1 decreased the conversion of B_2 into B_3 still further, so the $K_{a(\text{app})}$ decreased 14-fold, effectively abolishing its binding to DNA. In the case of p42 ETS1, it has a much reduced B_1 response, indicating that it is more difficult for p42 ETS1 to find its sequence-specific DNA, but once bound, it rapidly moves into the B_3 state because of a rapid conversion of the B_2 into the B_3 stable binding. Thus, the structural differences between p42 ETS1 and p51 ETS1 regulate the kinetic pathway to the B_3 state. It is interesting that the tryptophan fluorescence emission pattern differs for the p42 and p51 isoforms. There is fluorescence quenching of the p51 tryptophans when binding to the specific oligonucleotide and fluorescence enhancement of the tryptophans of the p42 ETS1 on specific oligonucleotide binding. This is evidence that the there is a conformational change in the ETS1 isoforms due to the lack of Exon VII. This model is currently undergoing further refinement in an effort to recover more information about the binding reaction from the BIAcore measurements.

Materials and methods

Instrumentation and reagents

The BIAcore instrument was manufactured by Pharmacia Biosensor AB (Uppsala, Sweden). Sensor chips CM5, Tween p20, and the amine coupling kit containing *N*-hydroxysuccinimide, *N*-ethyl-*N'*-(3-diethylaminopropyl)carbodiimide (EDC), and ethanolamine hydrochloride were from Pharmacia Biosensor AB.

Electrophoretic mobility shift assay

DNA sequence-specific binding of purified recombinant p51 ETS1 or purified recombinant p42 ETS1 was assessed by using EMSA. The purified ETS1 proteins were incubated with 250 ng of unlabeled probe for 30 min on ice in 4% glycerol, 1 mM EDTA, 5.0 mM dithiothreitol, 10 mM Tris-Cl, pH 7.5, and 1.0 mg/mL bovine serum albumin. The gels had 0.25× TBE (TBE = 89 mM Tris, 89 mM boric acid, and 1 mM EDTA), 5% glycerol, 1:1,000 (v/v) TEMED, and 14:1,000 (v/v) 5% ammonium persulfate; the electrode buffer was 0.25× TBE. The EMSA gels were prerun for 30 min at 250 V. Then, 20 μL of the sample was added and electrophoresis was continued for an additional 1.5 h. The EMSA gel was then soaked in ethidium bromide and observed under UV light.

Oligonucleotides

The oligonucleotides listed below were synthesized either with trityl group on or with a 5′ amino link. The trityl on oligonucleotides were purified by OPC chromatography according to Applied Biosystems' protocols.

1. 5′-TCGAGCCGGAAGTTCGA-3′ Wild type
2. 5′-TCGA**A**CCGGAAGTTCGA-3′ Mutant 1
3. 5′-TCGAGTCGGAAGTTCGA-3′ Mutant 2
4. 5′-TCGAGCTGGAAGTTCGA-3′ Mutant 3
5. 5′-TCGAGCC**A**GAAGTTCGA-3′ Mutant 4
6. 5′-TCGAGCCG**A**AAGTTCGA-3′ Mutant 5
7. 5′-TCGAGCCGGG**A**GTTCGA-3′ Mutant 6
8. 5′-TCGAGCCGGA**G**GTTCGA-3′ Mutant 7
9. 5′-TCGAGCCGGAAA**T**TCGA-3′ Mutant 8
10. 5′-TCGAGCCGGAAGC**T**CGA-3′ Mutant 9

Complementary oligonucleotides were dissolved in TE buffer (10 mM Tris-Cl, 0.5 mM EDTA, pH 7.4) and annealed, purified, and quantitated as described previously (Fisher et al., 1992). The oligonucleotides that had the 5′ amino group were biotinylated before annealing and purified from the unincorporated NHS-biotin by thin-layer chromatography.

Constructs, purification, and renaturation of p42 and p51 ETS1

The pET-15b expression vector (Novagen) and a modification of this vector termed SBpET+1, created by ligation of

```
GATCCCCGGGCA
    GGGCCCGTCTAG
```

into the *Bam* H1 cloning site, were utilized for these studies. The plasmid encoding p51 was generated by stepwise cloning of a *Ban-Hin* dIII fragment of pj10-2 (Watson et al., 1988) into the *Nde* 1 site of pET-15b. The plasmid encoding p42 was constructed by ligation of the *Ban* 1–*Hin* dIII fragment of pGemΔ7 into the *Sma* 1 site of SBpET+1. The pGemΔ7 was generated from a cDNA clone lacking Exon VII isolated from a λgt10 CEM library (Watson et al., 1988). The *Eco* R1 insert from this clone was substituted for the *Eco* R1–*Eco* R1 fragment in pGemJ10-2 and designated pGemΔ7. All of the constructs were verified by dideoxy DNA sequencing. The pet vectors carrying either p42 or p51 were grown to approximately 1 OD at 660 nm and induced by the addition of 1 mM ITPG and incubated for an additional 3 h before harvesting. The cell pellet was treated, sonicated, and washed with a sequential series of salts (Krippl et al., 1984) before final solubilization in 6 M guanidine-HCl and affinity purification on nickel sulfate chelate columns according to company protocols (Novagen). The fractions containing either p42 or p51 were reduced with 100 mM β-mercaptoethanol, acidified to pH 2.0 with 20% TFA, pumped directly onto a 10 × 25 × 100-mm C18 μ-Bondapak radial cartridge pak, developed with 0–35% acetonitrile gradient (30 min, 10 mL/min), and eluted as a single major peak with a 35–50% acetonitrile–0.05% TFA gradient (600 min, 1 mL/min). The fractions with p42 or p51 ETS1 were lyophilized and dissolved in 5 mL of 8 M guanidine-HCl, 40 mM Tris-HCl, pH 8.5, and 100 mM β-mercaptoethanol. The ETS1 proteins were renatured by passing the 5 mL of the reduced, guanidine-solubilized protein through a Pharmacia HiLoad 16/60 Superdex 75PG column equilibrated in BIAcore flow buffer at a flow rate of 0.2 mL/min. The renatured ETS protein comes out at the expected retention volume for a 42- or 51-kDa protein. The protein concentration for these samples was obtained by duplicate amino acid analysis after acid hydrolysis of the protein and was in the range of 1–10 μM.

CAM kinase II phosphorylation of p51 and p42 ETS1

Solutions (200 μL final volume) were made up of 50 mM Hepes, pH 7.3, 10 mM $MgCl_2$, 1 μM calmodulin, 0.4 mM ATP, 0.2 μM CAM kinase II, and either 320 nM p42 ETS1 or 120 nM p51 ETS1. Incubations were for 1 min at 30 °C in the presence of 0.5 mM $CaCl_2$ or 0.5 mM $CaCl_2$ plus 1 mM EGTA for the control sample. An injection of 20 μL of each sample was placed into the BIAcore at 8 μL/min.

Preparation of the sensor surface

Double-stranded oligonucleotides were prepared so that only the upper strand was biotinylated on the 5′ end. The CM5 sensor chip was modified streptavidin according to the BIAcore protocol. Sufficient DNA was injected onto the streptavidin-modified sensor chip to give the desired change of about 39 RUs (low-RU surface) or up to 800 RUs (high-RU surface). The surface concentrations of protein or DNA may be estimated by the following approximations: 1,000 RUs of protein is the equivalent of 1 ng of protein/mm^2 (BIAcore technical notes), and 800 RUs of DNA is the equivalent of 1 ng of DNA/mm^2 (BIAcore technical staff, pers. comm.).

Regeneration of the sensor surface

After binding of protein to the dsDNA, the binding surface could be regenerated to its original baseline with a pulse of 0.1%

SDS. Provided that all buffers were filter-sterilized and contained EDTA, we found that a binding surface could be used several hundred times over a period of more than 3 months. This provides a distinct advantage in that exactly the same DNA may be used and reused over an extended period.

BIAcore kinetic measurements

We used a low-RU surface so that the change in free protein concentration is not significantly affected by the binding reaction and follows Fick's Law. The p51 and p42 ETS1 proteins were equilibrated in the BIAcore flow buffer (10 mM Hepes, pH 7.3, 3.4 mM EDTA, 0.05% Tween 20, and 150 mM NaCl) to minimize the refractive index difference between the samples and flow buffer. A dilution series of p42 or p51 was made in the flow buffer, and 20 μL from each dilution was injected at 8 μL/min, followed by a 3-min washout and two 5-μL pulses of 0.1% SDS to remove the bound proteins from the surface for the next measurement.

Fluorimetric titrations

Fluorescence data were obtained using an SLM 48000S spectrofluorimeter equipped with double monochromators containing holographic gratings with 1,500 grooves/mm. Excitation was performed with a 450-W Xe arc lamp. Detection was accomplished with cooled red-sensitive photomultiplier tubes offset to null the dark counts. Readings were collected in the ratio mode using as a quantum counter a triangular quartz cell containing 3 g L^{-1} of rhodamine B solution. Excitation monochromator slits were set at 1-nm bandwidth, where sample photobleaching was undetectable. Emission monochromator slits were set to the appropriate resolution (usually at 4- or 8-nm bandwidth). Fluorimetric equilibrium binding isotherms for the binding of the p42 and p51 isoforms of human ETS1 protein to a double-stranded DNA oligonucleotide carrying its specific sequence were obtained at 25 °C in 10 mM Tris-Cl, pH 7.0, containing 0.1 mM EDTA and NaCl at a concentration ranging from 0 to 4 M. Samples were held in a dual-pathlength (0.2 × 1.0 cm) Suprasil quartz cuvette in a thermostated cell holder, with the narrow pathlength facing the excitation beam. Capped cells contained 300-μL samples. Data acquisition was performed by averaging 16 readings at fixed wavelength (340 nm, unless otherwise indicated). Titrations with acceptable signal-to-noise ratio could be carried out at ETS1 concentrations as low as 8 nM protein (ca. 60 nM Trp). A minimum of 8–10 aliquots of oligonucleotide (total volume, 30–40 μL) at the appropriate concentration in the above buffer were added until the protein fluorescence emission intensity showed no further change; background fluorescence was subtracted and readings were corrected for dilution effects. Inner filter effects due to oligonucleotide absorbance were negligible at the concentrations used. Data were processed by an IBM-PC/XT computer. Titrations were plotted as relative fluorescence (F/F_0) vs. [oligo]/[ETS1] ratio, where F_0 and F are the fluorescence emission intensity (in arbitrary units) at the beginning and during the titration, respectively, and the concentrations of oligonucleotide and protein are expressed as the molarity of oligonucleotide molecules and protein monomers, respectively. Titrations were analyzed according to the Langmuir model, which assumes independent ligand association with a single binding site and seems justified by the 1:1 stoichiometry observed from the titrations. Binding affinities were calculated either from the fractional saturation (θ) at the stoichiometric point, using the expression $K_{app} = \theta/[(1-\theta)^2 \cdot P^{-1}]$, where P is the protein concentration at the stoichiometric point, or from double-reciprocal plots of $1/\Delta F$ vs. $1/[\text{oligo}]_{free}$, where ΔF is $(F_0 - F)/F_0$. Double-reciprocal plots yield a straight line whose y-intercept represents the reciprocal of the limiting fluorescence quenching (Q_{max}) or enhancement (E_{max}), and whose slope is the reciprocal of K_{app}. Salt-back titrations were carried out by addition of aliquots of a 5 M NaCl solution to a preformed ETS1–oligo complex. The salt dependence of the binding reflects the net ion displacement in the association reaction, $d(\log K)/d(\log [Na^+]) = m' \cdot Y + k$, where m' is the number of ion pairs formed, Y is the fraction of counterion thermodynamically bound per nucleic acid phosphate, and k is the number of anions displaced in the binding reaction (Record et al., 1976); Y is 0.70 for double-stranded DNA. A so-called double-logarithmic plot of log K_{app} vs. log $[Na^+]$ yields a straight line whose slope characterizes the salt dependence of the interaction and whose abscissa intercept measures the binding free energy at the reference state of 1 M Na^+ (corresponding to the nonelectrostatic component of the binding interactions).

Analysis and modeling

The system of first-order nonlinear differential equations we use to mathematically describe our model is shown in Equation 1. The first entry in the system described delivery of protein through the boundary layer and into the dextran matrix. The next 3 entries describe the 3 states of bound complexes that are observed experimentally. The last entry describes polymerization of bound protein.

$$\begin{bmatrix} dF/dt \\ dB_1/dt \\ dB_2/dt \\ dB_3/dt \\ dD/dt \end{bmatrix} = \begin{bmatrix} k_{diff}\{C[1-\Phi(t-\tau)] - F\} \\ k_+(R - B_1 - B_2 - B_3)F - k_- B_1 - k_{12}B_1 \\ k_{12}B_1 - k_{23}B_2 - k_{2-}B_2 \\ k_{23}B_2 - k_{3-}B_3 \\ p_1(B_1 + B_2 + B_3 - P_1 D)F - p_2 D \end{bmatrix}, \quad (1)$$

where Φ is the Heaviside step function, R is the initial number of binding sites in RUs, C is the concentration of protein in the flow in g/L, and k_i and p_i have the meanings shown in Figure 5.

The observed RU signal is modeled by the total amount of protein that leaves solution and resides on the DNA within the dextran matrix:

$$RU_{bound}(t) = B_1(t) + B_2(t) + B_3(t). \quad (2)$$

Examination of this model shows that the diffusion term (the first equation in the system of Equation 1) provides a simplified description of material transport to and from the dextran matrix. This description holds when the binding reaction has a minimal effect on the time course of diffusion. The effect of steric hindrance on binding is likewise not included in the model. Both the simple description of diffusion and the lack of steric effects in the model limit its use to surfaces with only low levels of DNA attached to the sensor chip (<50 RUs).

To compare the measured reaction rate with the model, data were first normalized to a zero baseline by averaging several measurements occurring just before the injection, and taking this average RU value as that corresponding to no bound protein. In the event of baseline drift with changing flow concentration, somewhat more complex normalization procedures were applied.

The entire time sequence of normalized data (protein injection and washout), for several concentration values, is fitted to the model in a least-squares sense. The proposed model provides a description of an entire time course of the experiment consisting of a series of injection and washout cycles at various protein concentrations. Attempting to fit this model to a single cycle (just 1 protein concentration) produces numerically unstable results, that is, for a single cycle, this model appears to be overparameterized. However, when we demand that the model has physical reality (i.e., positive rate constants) and require the model to describe the data in 3 experimental dimensions (time, flow concentration, and RU signal), unique parameter estimates are obtained. Global fitting allowed us to reject binding models that fit satisfactorily individual concentration time progressions.

Newton iterative procedure

The fitting procedure, written using MATLAB, numerically integrates the differential system (Equation 1) iteratively to compute approximate derivatives of the parameters, then updates the parameter estimates using a Gauss–Newton iterative method. The current version of the MATLAB program runs on a CONVEX supercomputer and executes about 200 million floating point operations per fit (a copy is available from the authors upon request).

Acknowledgments

We thank Dr. Thomas J. Soderling for the generous gift of CAM kinase II, Dr. Raymond V. Gilden for his support in obtaining the BIAcore equipment, Karen Larson-McNitt for programming assistance, Drs. Louis Henderson and Raymond Sowder for amino acid analysis, and members of the Laboratory of Molecular Oncology for constructive discussions of this work. The contents of this publication do not necessarily reflect the views or policies of the Department of Health and Human Services, nor does mention of trade names, commercial products, or organizations imply endorsement by the US government.

References

Andrade JD, Hlady V. 1986. Protein adsorption and materials biocompatibility: A tutorial review and suggested hypothesis. *Adv Polymer Sci 79*:1–63.

Fisher RJ, Koizumi S, Kondoh A, Mariano JM, Mavrothalassitis G, Bhat NK, Papas TS. 1992. Human ETS1 oncoprotein: Purification, isoforms, -SH modification, and DNA sequence-specific binding. *J Biol Chem 267*:17957–17965.

Fisher RJ, Mavrothalassitis G, Kondoh A, Papas TS. 1991. High-affinity DNA-protein interactions of the cellular ETS1 protein: The determination of the ETS binding motif. *Oncogene 6*:2249–2254.

Fleischman LF, Pilaro AM, Murakami K, Kondoh A, Fisher RJ, Papas TS. 1993. c-Ets-1 protein is hyperphosphorylated during mitosis. *Oncogene 8*:771–780.

Gegonne A, Punyammalee B, Rabault B, Bosselut R, Seneca S, Crabeel M, Ghysdael J. 1992. Analysis of the DNA binding and transcriptional activation properties of the Ets1 oncoprotein. *New Biol 4*:512–519.

Hagman J, Grosschedl R. 1992. An inhibitory carboxyl-terminal domain in Ets-1 and Ets-2 mediates differential binding of ETS family factors to promoter sequences of the mb-1 gene. *Proc Natl Acad Sci USA 89*:8889–8893.

Hill CS, Marais R, John S, Wynne J, Dalton S, Treisman R. 1993. Functional analysis of a growth factor-responsive transcription factor complex. *Cell 73*:395–406.

Ho IC, Bhat NK, Gottschalk LR, Lindsten T, Thompson CB, Papas TS, Leiden JM. 1990. Sequence-specific binding of human Ets-1 to the T cell receptor alpha gene enhancer. *Science 250*:814–818.

Jorcyk CL, Watson DK, Mavrothalassitis GJ, Papas TS. 1991. The human ETS1 gene: Genomic structure, promoter characterization and alternative splicing. *Oncogene 6*:523–532.

Koizumi S, Fisher RJ, Fujiwara S, Jorcyk C, Bhat NK, Seth A, Papas TS. 1990. Isoforms of the human ets-1 protein: Generation by alternative splicing and differential phosphorylation. *Oncogene 5*:675–681.

Krippl B, Ferguson B, Rosenberg M, Westphal H. 1984. Functions of purified EIA protein microinjected into mammalian cells. *Proc Natl Acad Sci USA 81*:6988–6992.

Lim F, Kraut N, Framptom J, Graf T. 1992. DNA binding by c-ets-1, but not v-ets, is repressed by an intramolecular mechanism. *EMBO J 11*:643–652.

Liu X, Miller CW, Koeffler PH, Berk AJ. 1993. The p53 activation domain binds the TATA box-binding polypeptide in holo-TFIID, and a neighboring p53 domain inhibits transcription. *Mol Cell Biol 13*:3291–3300.

Lofas S, Johnsson B. 1990. A novel Hydrogel matrix on gold surfaces in surface plasmon resonance sensors for fast and efficient covalent immobilization of ligands. *J Chem Soc Chem Commun 21*:1526–1528.

Lohman TM, Bujalowski W. 1991. Thermodynamic methods for model-independent determination of equilibrium binding isotherms for protein–DNA interactions: Spectroscopic approaches to monitor binding. *Methods Enzymol 208*:258–290.

Lok BK, Cheng Y-L, Robertson CR. 1983. Protein adsorption on crosslinked polydimethylsiloxane using total internal reflection fluorescence. *J Colloid Interface Sci 91*:104–116.

Mavrothalassitis G, Fisher RJ, Symth F, Watson DK, Papas TS. 1994. Inferences regarding the structure of the ETS1 DNA-binding domain as determined by mutational analysis. *Oncogene*. Forthcoming.

Nelson B, Tian G, Erman B, Gregoire J, Maki R, Sen R. 1993. Regulation of lymphoid-specific immunoglobulin mu heavy chain gene enhancer by ETS-domain proteins. *Science 261*:82–86.

Nikolov DB, Hu SH, Lin J, Gasch A, Hoffmann A, Horikoshi M, Chua NH, Roeder RG, Burley SK. 1992. Crystal structure of TFIID TATA-box binding protein. *Nature 360*:40–46.

Nye JA, Petersen JM, Gunther CV, Jonsen MD, Graves BJ. 1992. Interaction of murine ets-1 with GGA-binding sites establishes the ETS domain as a new DNA-binding motif. *Genes Dev 6*:975–990.

Pognonec P, Boulukos KE, Bosselut R, Boyer C, Schmitt VA, Ghysdael J. 1990. Identification of a Ets1 variant protein unaffected in its chromatin and in vitro DNA binding capacities by T cell antigen receptor triggering and intracellular calcium rises. *Oncogene 5*:603–610.

Pongubala JMR, van Beveren C, Nagulapalli S, Klemsz MJ, McKercher SR, Maki RA, Atchison ML. 1993. Effect of PU.1 phosphorylation of interaction with NF-EM5 and transcriptional activation. *Science 259*:1622–1625.

Pugh BF, Tjian R. 1992. Diverse transcriptional functions of the multisubunit eukaryotic TFIID. *J Biol Chem 267*:679–682.

Record MT, Ha JH, Fisher MA. 1991. Analysis of equilibrium and kinetic measurements and mechanism of formation of site-specific complexes between proteins and helical DNA. *Methods Enzymol 208*:291–343.

Record MT Jr, Lohman TM, de Haseth P. 1976. Ion effects on ligand–nucleic acid interactions. *J Mol Biol 107*:145–158.

Seth A, Ascione R, Fisher RJ, Mavrothalassitis GJ, Bhat NK, Papas TS. 1992. The ETS gene family. *Cell Growth Differ 3*:327–334.

Thompson CC, Brown TA, McKnight SL. 1991. Convergence of Ets- and notch-related structural motifs in a heteromeric DNA binding complex. *Science 253*:762–768.

Wasylyk B, Wasylyk C, Flores P, Begue A, Leprince D, Stehelin D. 1990. The c-ets proto-oncogenes encode transcription factors that cooperate with c-Fos and c-Jun for transcriptional activation. *Nature 346*:191–193.

Wasylyk C, Kerckaert JP, Wasylyk B. 1992. A novel modulator domain of Ets transcription factors. *Genes Dev 6*:965–974.

Watson DK, McWilliams MJ, Lapis P, Lautenberger JA, Schweinfest CW, Papas TS. 1988. Mammalian ets-1 and ets-2 genes encode highly conserved proteins. *Proc Natl Acad Sci USA 85*:7862–7866.

Zawel L, Reinberg D. 1993. Initiation of transcription by RNA polymerase II: A multi-step process. *Progr Nucleic Acid Res Mol Biol 44*:67–108.